The Microphysical Feedback of Cirrus Cloud in Climate Change

By Tsuneaki Suzuki, Masayuki Tanaka

Center for Atmospheric and Oceanic Studies, Faculty of Science, Tohoku University, Sendai 980, Japan

and

Teruyuki Nakajima

Center for Climate System Research, University of Tokyo, Meguro-ku, Tokyo 153, Japan
(Manuscript received 26 April 1993, in revised form 14 September 1993)

Abstract

The feedback effects of cirrus clouds in climate change are investigated, taking account of the temperature dependence of both ice water content and size distribution. The sensitivity parameter which is defined as a sum of partial derivatives is calculated with an accurate radiation code applying the 4-stream discrete-ordinates method and the method of exponential-sum fitting for gaseous transmission (ESFT). Microphysical properties of cirrus clouds are parameterized in terms of the cloud temperature from the data of aircraft observations. The value of $\partial H/\partial[IWC] \times \partial[IWC]/\partial T$, *i.e.*, a product of partial derivatives associated with ice water content feedback, is estimated to be 1.3–2.3 W m^{-2}°C^{-1}, meaning a positive feedback effect, and the value of $\partial H/\partial[SD] \times \partial[SD]/\partial T$ which is associated with size distribution feedback is estimated to be -0.1–-1.8 W m^{-2}°C^{-1}, meaning a negative feedback effect. The positive ice water content feedback is significantly cancelled by the negative size distribution feedback especially at cloud temperature in the vicinity of -45°C. It is thus shown that the temperature dependence not only of ice water content but also of size distribution is important to estimate the microphysical feedback of cirrus cloud.

1. Introduction

Many researchers studied the effect of cloud microphysical feedback on climate change by means of radiative convective models (Charlock, 1982; Somerville and Remer, 1984; Schlesinger and Roeckner, 1988; Stephens *et al.*, 1990) and general circulation models (Roeckner *et al.*, 1987; Cess *et al.*, 1990; Slingo, 1990). In spite of these efforts, we have not yet understood whether the microphysical feedback of cloud system is positive or negative. In particular, evaluation of cirrus cloud microphysical feedback is difficult due not only to the complexity of microphysical processes, but also to its delicate radiative balance. As most cirrus clouds do not behave as black bodies, their infrared radiative properties vary with a change of microphysical properties. Changes of both solar and infrared radiative properties caused by a change in microphysics thus induce climate feedbacks which have opposite signs for the respective wavelength regions. Charlock (1982) showed that the sign of the ice water content (IWC) feedback depends on the initial value of the IWC. Stephens *et al.* (1990) showed that the sign of the IWC feedback also depends on the choice of particle sizes. These studies, however, adopted an emissivity approximation which is valid only for isothermal and non-scattering media. In this respect, Stephens (1980) pointed out that the contribution of scattering to the radiative transfer in cirrus clouds is significant even in the infrared region. Stackhouse and Stephens (1991) successfully applied a two-stream radiative transfer code which includes scattering in the infrared region to the explanation of the observed optical properties of cirrus clouds. Such a careful treatment of the radiative transfer is also desired, especially in the infrared region, for the estimation of microphysical feedbacks of cirrus clouds.

Moreover, most of the above-mentioned theoretical studies were devoted to the effect of temperature dependence of the IWC (IWC feedback) without considering the effect of temperature dependence of the size distribution. The size distribution, however, affects significantly the radiative properties of cirrus clouds as in Stephens *et al.* (1990). Foot (1988)

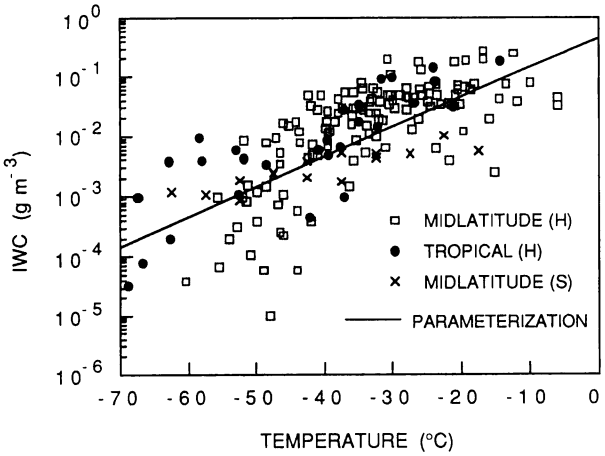

Fig. 1. Cloud temperature versus ice water content. Symbols are as follows: squares, mid-latitude cirrus clouds (after Heymsfield and Donner, 1990); circles, tropical cirrus clouds (after Heymsfield and Donner, 1990); crosses, mid-latitude cirrus clouds (after Sassen *et al.*, 1989). Solid line shows our parameterization.

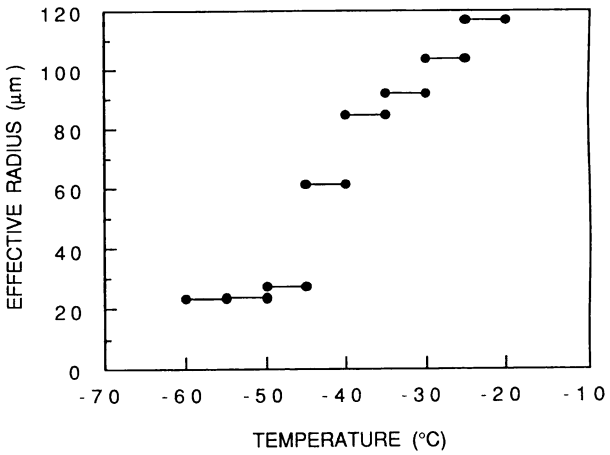

Fig. 2. Cloud temperature versus effective radius of cloud particle.

showed from aircraft observations that the infrared optical thickness of cirrus clouds is closely related to the size distribution. Recent airborne measurements have revealed the fact that the size distribution of cirrus clouds depends strongly on the cloud temperature (Heymsfield and Platt, 1984; Sassen *et al.*, 1989). Such temperature dependence of the size distribution is also expected to induce a significant feedback mechanism through the change of cloud optical properties (size distribution feedback).

The aim of this paper is to study microphysical feedbacks of cirrus clouds taking account of the temperature dependence of both IWC and size distribution by use of a radiation code with reasonable accuracy. In the next section, the IWC and the size distribution of cirrus clouds are parameterized in terms of cloud temperature from the data of airborne measurement. Section 3 describes the method used for evaluating feedback processes. A sensitivity parameter ratio, which is defined as a ratio of temperature change derived by considering a feedback process to that without the feedback, is expressed in terms of partial derivatives related to respective feedback mechanisms. The magnitudes of cirrus cloud feedbacks are evaluated numerically in Section 4 and discussed in Section 5.

2. Parameterizations of the microphysical properties of cirrus clouds

2.1 Temperature dependence of IWC

Figure 1 shows the relationship between cirrus cloud temperature and IWC. Plotted data were measured in mid-latitude cirrus clouds associated with warm frontal overrunning systems, warm frontal occlusions, upper-level closed lows, and jet stream bands (Heymsfield and Donner, 1990; Sassen *et al.*, 1989), and in tropical cirrus clouds which were observed at locations free from deep convective clouds (Heymsfield and Donner, 1990). The data obtained by Heymsfield and Donner (1990) for mid-latitude and tropical cirrus clouds show very similar temperature dependence with each other, though the data points scatter rather widely. The data by Sassen *et al.* (1989) show a little smaller temperature dependence than those by Heymsfield and Donner (1990). The following empirical relationship between IWC and cloud temperature is obtained from mid-latitudes-tropics combined data,

$$w\left(\mathrm{g\,m^{-3}}\right) = 1.371 \times 10^{-14+4.962\times10^{-2}\times(273+T(^{\circ}\mathrm{C}))}. \quad (1)$$

2.2 Temperature dependence of size distribution

The size distributions of cirrus clouds summarized by Heymsfield and Platt (1984) for warm frontal systems are adopted in this study. Heymsfield and Platt (1984) showed the size distributions averaged for each 5°C temperature interval from −20 to −60°C. They also showed that spatial crystals such as bullet rosettes are predominant in the temperature range from −20 to −40°C, while columns are predominant at temperatures bellow −50°C. In the temperature range from −40 to −50°C, predominant ice crystal habits depend on the convective activity of cirrus clouds: spatial and columnar crystals predominate in convective and in stable cirrus clouds, respectively.

For the purpose of calculating single-scattering properties, ice crystal habits are treated as volume-equivalent spheres in this study, though Heymsfield and Platt (1984) represented their size distribution data in terms of the maximum dimension of ice crystals. The radius of a volume equivalent sphere r_{eq}

is related to the maximum dimension L as follows, so that the size distributions for volume-equivalent spheres can be obtained from the observed size distribution data. The ice crystal habits are assumed to be bullet rosettes for temperatures higher than −45°C, and columns for temperatures lower than −45°C. The mass of an ice crystal M is related to the radius of the volume-equivalent sphere by

$$M = \frac{4}{3}\pi r_{eq}^3 \rho. \tag{2}$$

Assuming a constant ice crystal density ρ of 0.78 g cm^{-3} (Heymsfield, 1972), the relationships between L and r_{eq} are given by

$$r_{eq}(\mu\text{m}) = 238 \times L(\text{mm}), \tag{3}$$

for the bullet rosette, and

$$r_{eq}(\mu\text{m}) = 173 \times L^{0.57}(\text{mm}), \tag{4}$$

for columns, from the relationships between M and L for each crystal habit (Heymsfield, 1977). Figure 2 shows the effective radius of the cirrus cloud particles thus obtained, *i.e.*,

$$r_{eff} = \frac{\int_{r_{eq}^{\min}}^{r_{eq}^{\max}} n(r_{eq}) r_{eq}^3 dr_{eq}}{\int_{r_{eq}^{\min}}^{r_{eq}^{\max}} n(r_{eq}) r_{eq}^2 dr_{eq}}, \tag{5}$$

from the data, where $n(r_{eq})$ is the size distribution for the volume-equivalent spheres, and $r_{eq}^{\max}$ and $r_{eq}^{\min}$ are the maximum and minimum values of the equivalent radius of cloud particles, respectively. The effective radius of cloud particles increases with an increase of the cloud temperature. The change of crystal habit causes the discontinuous change of the effective radius in the vicinity of −45°C. The size distributions are normalized by the values of IWC before calculating single-scattering properties of cirrus clouds.

3. Method of evaluating the feedback processes

The magnitude of climate feedback is described in terms of partial derivatives as in Schlesinger and Mitchell (1987). The change of net radiative flux at the tropopause, ΔH, is defined by

$$\Delta H = \Delta F + \Delta Q, \tag{6}$$

where ΔF and ΔQ are respective changes of net infrared and net solar fluxes at the tropopause (both downward positive). Assuming that the net radiative flux at the tropopause is affected by an external perturbation, direct response to tropospheric temperature change and indirect response to changes of internal factors due to tropospheric temperature change, we have

$$\Delta H = \frac{\partial H}{\partial [EXT]} \Delta [EXT] + \left\{ \frac{\partial H}{\partial T} + \sum_i \frac{\partial H}{\partial [FB]_i} \frac{\partial [FB]_i}{\partial T} \right\} \Delta T, \tag{7}$$

where $[EXT]$ is the quantity related to external perturbation, for instance CO_2 concentration, T is the surface temperature, and $[FB]_i$ are quantities related to climate feedbacks, which are expected to change due to the external perturbation, *i.e.*, the water vapor concentration $[H_2O]$, the ice water content of cirrus cloud $[IWC]$ and the size distribution of cloud particles $[SD]$. We assume that the lapse rate of tropospheric temperature is invariant throughout climatic changes, so that the tropospheric temperature changes in parallel with the surface temperature.

If the climate system reaches a new equilibrium state, the value of ΔH vanishes as

$$\Delta H = 0. \tag{8}$$

From Eq. (7) and (8), the temperature change caused by an external perturbation is given by

$$\Delta T = \frac{-\dfrac{\partial H}{\partial [EXT]} \Delta [EXT]}{\lambda \left(\sum_i FB_i \right)}, \tag{9}$$

where the sensitivity parameter λ is defined as

$$\lambda \left(\sum_i FB_i \right) = \frac{\partial H}{\partial T} + \sum_i \frac{\partial H}{\partial [FB]_i} \frac{\partial [FB]_i}{\partial T}. \tag{10}$$

The terms related to each climate feedback appear in Eq. (10) as partial derivatives. This means that the effect of each climate feedback can be evaluated independently from Eq. (9) and (10), neglecting interactions between different feedbacks. The partial derivative $\partial H/\partial X$ (X being T or $[FB]_i$) is calculated by holding all variables except for X constant at an initial unperturbed state.

Now, we introduce the sensitivity parameter ratio as an index of magnitude of the climate feedback, which is the ratio of the temperature change calculated with considering the feedback process (ΔT) to that without considering the feedback process (ΔT_0),

$$R \left(\sum_i FB_i \right) = \frac{\Delta T}{\Delta T_0} = \frac{\lambda_0}{\lambda \left(\sum_i FB_i \right)}, \tag{11}$$

where

$$\Delta T_0 = \frac{-\frac{\partial H}{\partial [EXT]}\Delta [EXT]}{\lambda_0}, \tag{12}$$

and

$$\lambda_0 = \frac{\partial H}{\partial T}. \tag{13}$$

If the sensitivity parameter ratio is larger than unity, the feedback is positive, and vice versa. For a partially cloudy atmosphere with cloud amount A_D, the sensitivity parameter ratio R_{PC} which includes both water vapor feedback and microphysical feedbacks of cirrus cloud, is defined by

$$R_{PC}\left(H_2O + \sum_i CFB_i\right) = \frac{A_D\lambda_{0D} + (1 - A_D)\,\lambda_{0R}}{A_D\lambda_D\left(H_2O + \sum_i CFB_i\right) + (1 - A_D)\,\lambda_R\,(H_2O)}, \tag{14}$$

where CFB_i denotes either the IWC feedback or the size distribution feedback. The subscripts D and R refer to the quantities for overcast and clear atmospheres, respectively, and the value of ΔH for the partially cloudy atmosphere is assumed to be given by

$$\Delta H = A_D\Delta H_D + (1 - A_D)\,\Delta H_R. \tag{15}$$

4. Evaluation of cirrus cloud microphysical feedbacks

4.1 Model description

4.1.1 Radiation treatment

In this study, both solar and infrared radiative transfer in cloudy atmospheres are calculated by the discrete-ordinates and the matrix-operator combined method (Nakajima and Tanaka, 1986). This method is formulated originally for the transfer of solar radiation, so that it is extended to the transfer of infrared radiation. The Planck function in the thermal emission term is approximated by a linear function of optical thickness within the cloud layer, while it is fitted by third-order polynomials of the optical thickness outside the cloud layer. A 4-stream approximation is adopted to calculate radiative fluxes applying 2-point shifted-Gauss quadrature formula to each hemisphere. Single scattering properties of cloud particles are determined from Mie theory by adopting the refractive index of ice compiled by Warren (1984). The phase function is truncated by the delta-M method (Wiscombe, 1977). Thus, the discrete-ordinates part of our method which is applied to each homogeneous sublayer, is closely similar to the delta-four-stream approximation developed by Liou *et al.* (1988). They also examined the accuracy of the delta-four-stream approximation for various asymmetry factors, single scattering albedos, optical depths and solar zenith angles, and showed that reflected and transmitted fluxes of solar radiation can generally be estimated from the approximation with an accuracy better than ±5 %. The infrared flux calculated by the same approximation is expected to be more accurate, because the infrared radiation is more isotropic than the solar radiation.

The gaseous absorption is included by means of the method of exponential-sum fitting for gaseous transmission (ESFT) developed by Shi (1981). This method can treat overlapping of absorption bands of different constituents by multiple-sum formulae, and take account of the temperature and pressure dependence of absorption coefficients accurately from the ground to as high as 0.1 mb. The ESFT absorption coefficients are prepared for the wavelength range from 0.69 μm to the microwave region. The solar spectrum (from 0.69 to 4.2 μm) is divided into 17 intervals and infrared spectrum (larger than 4.2 μm) is divided into 21 intervals. Water vapor, CO_2 and O_3 are incorporated as absorption gases as shown in Table 1. The absorption of O_3 in the ranges from 0.20 to 0.36 μm and 0.41 to 0.69 μm is taken from the World Meteorological Organization (1985) and divided into a total of 102 intervals. The continuum absorption of water vapor from 8 to 12 μm is also incorporated (Roberts *et al.*, 1976). Rayleigh scattering is considered in the wavelength region from 0.2 to 0.69 μm.

4.1.2 Atmospheric models

An atmosphere closely similar to that obtained by Manabe and Wetherald (1967) from a radiative-convective model is adopted as an initial atmosphere. The vertical temperature profile is just the same as the result of the radiative convective model by Manabe and Wetherald (1967); the ground temperature is given to be 288.39 K. The relative humidity outside cloud layer is also adopted from Manabe and Wetherald (1967), and assumed to be conservative throughout climate changes. The water vapor in the cloud layer is assumed to be saturated at the given temperature. The CO_2 concentration of 300 ppmv is also adopted from Manabe and Wetherald (1967). Though this CO_2 concentration is a little smaller than the recent value of 350 ppmv, the evaluation of the sensitivity parameter described in Section 3 is not so sensitive to the concentration of CO_2. The ozone column and its vertical distribution are adopted from the U.S. standard atmosphere. The surface albedo and the cosine of solar zenith angle are assumed to be 0.1 and 0.5, respectively. The solar constant of 1367 W m^{-2} is adopted from Fröhlich and London (1986). The model atmosphere is divided into thirty layers; the top ten layers have each

Table 1. Solar and infrared absorption bands taken into account in this radiative transfer model. Bands with asterisks are incorporated by ESFT method.

Absorption gas	Infrared		Solar	
	Spectral range (cm^{-1})	Number of band divisions	Spectral range (cm^{-1})	Number of band divisions
H_2O	0–2380*	21	2380–11300*	13
			11660–12740*	1
			13400–14500*	1
CO_2	530–1110*	5	2380–2680*	1
	1200–1430*	2	3080–3890*	2
	1810–2380*	2	4540–5370*	1
			5920–6990*	2
			8040–8310*	1
O_3	610–810*	2	14500–24540	46
	940–1200*	2	27586–50000	56

3 km thickness, the middle ten layers have each 1 km thickness and the bottom ten layers have each 0.5 km thickness.

Dowling and Radke (1990) summarized many observations of the thickness and the altitude of cirrus clouds. They showed that measured thicknesses of cirrus cloud are ranging from 0.1 to 8 km with the typical thickness of 1.5 km. They also showed that measured altitudes of cloud center are ranging from 4 to 20 km, and suggested that typical cloud-center altitudes of cirrus clouds are about three quarters of the local tropopause height. In this study, a single cloud layer with thickness from 1 to 3 km is embedded in the upper troposphere between 6 and 11 km altitude, and its microphysical properties are calculated with the parameterization given in Section 2 unless specified. The microphysical properties are assumed to be homogeneous within the layer of 1 km thickness. For the cirrus cloud thicker than 1 km, the cloud layer is divided into 1 km-thick sublayers, and the microphysical properties are assumed to be homogeneous for the respective sub-layers. It is also assumed that the cloud altitude is invariant throughout climate change.

Although these atmospheric models do not strictly satisfy the radiative-convective equilibrium which is assumed in the definition of the sensitivity parameter in Section 3, the magnitudes of microphysical feedbacks are not significantly affected by use of such model atmospheres (see 5.3). The partial derivatives composing the sensitivity parameter are calculated by increasing the tropospheric temperature by 5°C, corresponding to the temperature interval adopted by Heymsfield and Platt (1984) (see Fig. 2). The height of the tropopause is fixed at 15 km for these calculations.

4.2 Evaluation of feedback processes

4.2.1 Evaluation of partial derivatives

First, the partial derivatives related to each feedback mechanism are evaluated for an overcast cirrus with 1 km thickness. Cloud top altitude is in the range from 7 to 11 km. The partial derivative related to the direct temperature response (*i.e.*, $\partial H/\partial T$) is obtained in the range from -3.5 to $-3.7\,\mathrm{W\,m^{-2}{}^{\circ}C^{-1}}$. The product of partial derivatives related to the water vapor feedback (*i.e.*, $\partial H/\partial[H_2O]\times\partial[H_2O]/\partial T$) is obtained in the range from 1.1 to $1.3\,\mathrm{W\,m^{-2}{}^{\circ}C^{-1}}$. If the water vapor increases with increasing tropospheric temperature, an increase of radiation absorption in the troposphere suppresses the upward radiative flux at the tropopause for both solar and infrared radiations. The increase of water vapor thus enhances the increase of temperature; the water vapor feedback is positive for all wavelength regions. The value of $\partial H/\partial[H_2O]\times\partial[H_2O]/\partial T$ for the infrared radiation ranges from 1.0 to $1.2\,\mathrm{W\,m^{-2}{}^{\circ}C^{-1}}$, and these values are much larger than the value of $0.1\,\mathrm{W\,m^{-2}{}^{\circ}C^{-1}}$ of the corresponding quantity for the solar radiation. Schlesinger and Mitchell (1987) estimated that the values of $\partial H/\partial T$ and $\partial H/\partial[H_2O]\times\partial[H_2O]/\partial T$ are to be $-3.3\,\mathrm{W\,m^{-2}{}^{\circ}C^{-1}}$ and in the range from 1.0 to $1.3\,\mathrm{W\,m^{-2}{}^{\circ}C^{-1}}$, respectively, from their model simulations where these derivatives are derived from differences between two (*i.e.*, initial and newly established) equilibrium states. The close agreement between Schlesinger and Mitchell (1987) and our estimations espouses the validity of our convenient calculation of the partial derivatives related to climate feedbacks.

The product of partial derivatives related to the cirrus cloud IWC (*i.e.*, $\partial H/\partial[IWC]\times\partial[IWC]/\partial T$) ranges from 1.3 to $1.8\,\mathrm{W\,m^{-2}{}^{\circ}C^{-1}}$, as large as the quantity $\partial H/\partial[H_2O]\times\partial[H_2O]/\partial T$ as shown in Fig.

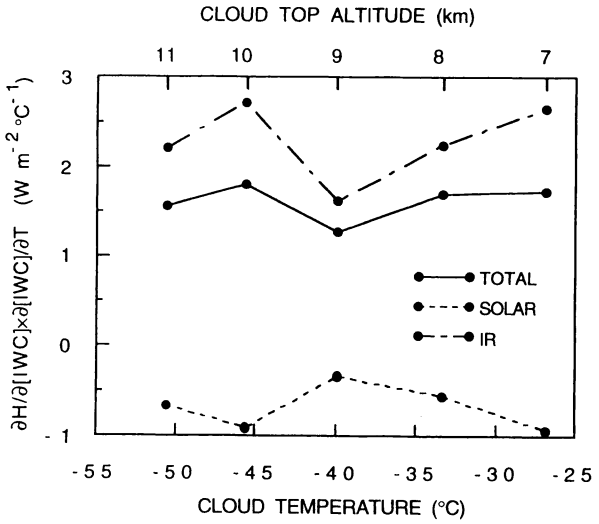

Fig. 3. Partial derivatives related to ice water content feedback (solid line), its solar component (broken line) and infrared component (dash-dot line) as a function of cloud temperature (cloud top altitude).

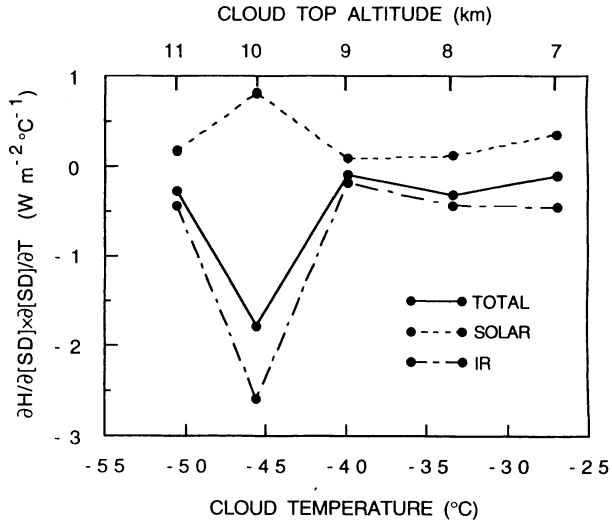

Fig. 4. Same as Fig. 3, except for partial derivatives related to size distribution feedback.

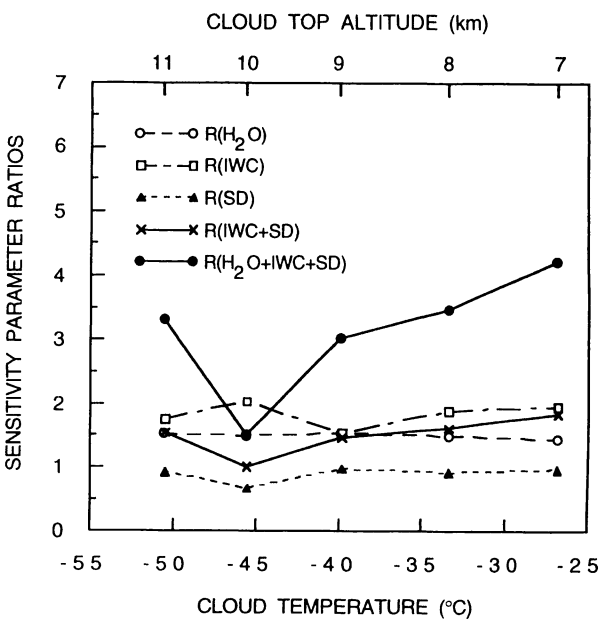

Fig. 5. Sensitivity parameter ratios for respective feedbacks: water vapor feedback (H_2O), ice water content feedback (IWC), size distribution feedback (SD), and their combinations ($IWC+SD$, $H_2O+IWC+SD$).

3. Because cirrus clouds become more opaque due to the increase of IWC, the net downward solar radiation decreases and the net downward infrared radiation increases at the tropopause with increasing temperature. The increase of IWC thus suppresses energy gain at tropopause for the solar radiation and vise versa for the infrared radiation; the IWC feedback is negative for the solar spectral region and positive for the infrared region. The total magnitude of the IWC feedback, *i.e.*, the sum of the feedbacks for both solar and infrared radiations, is positive at the cloud top altitude from 7 to 11 km. The product of partial derivatives related to the size distribution of cirrus cloud (*i.e.*, $\partial H/\partial[SD] \times \partial[SD]/\partial T$) varies from -0.1 to $-1.8\,\mathrm{W\,m^{-2}{}^{\circ}C^{-1}}$ as shown in Fig. 4. The large variability of $\partial H/\partial[SD] \times \partial[SD]/\partial T$ at the cloud top altitude of 10 km results from the drastic change of the size distribution at that altitude (temperature) mentioned in Section 2.2. As temperature increases, the particle sizes become larger and cirrus clouds become more transparent for a fixed value of IWC. Consequently, the net downward fluxes at the tropopause increase and decrease for the solar and the infrared radiations, respectively. The size distribution feedback is therefore positive for the solar radiation, and is negative for the infrared radiation. The total magnitude of the size distribution feedback is negative due to the large negative feedback for the infrared radiation.

4.2.2 Evaluation of sensitivity parameter ratio

Figure 5 shows the relationship between the sensitivity parameter ratios and the cloud-top altitude. The sensitivity parameter ratios are calculated from the partial derivatives discussed in Section 4.2.1 for an overcast cirrus cloud with 1 km thickness. Values of the sensitivity parameter ratio $R(IWC)$ including only the IWC feedback are estimated to be 1.5–2.0; the temperature change is amplified by a factor 1.5–2.0 due to the IWC feedback. The sensitivity parameter ratio $R(SD)$, which includes only the size distribution feedback, is slightly smaller than unity; the temperature dependence of the size distribution by

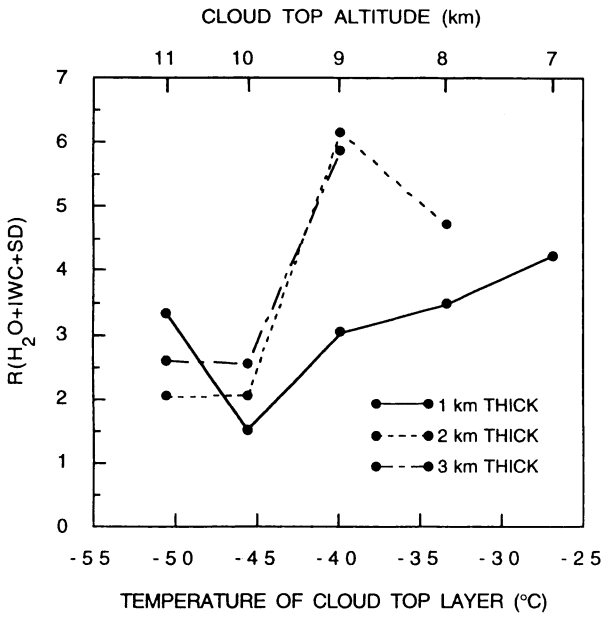

Fig. 6. Sensitivity parameter ratio $R(H_2O+IWC+SD)$ versus temperature of the cloud-top layer for three different cloud thicknesses.

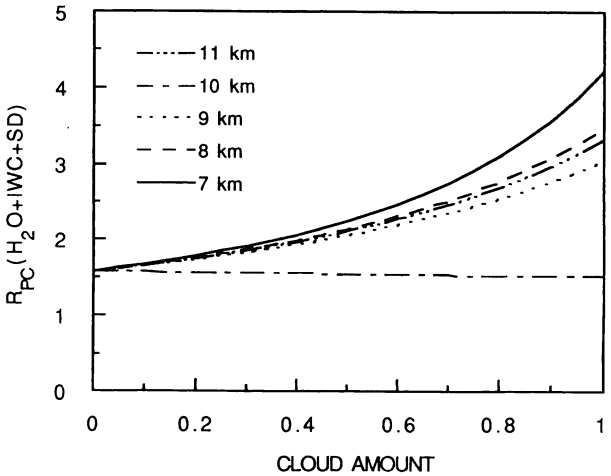

Fig. 7. Sensitivity parameter ratio $R_{PC}(H_2O+IWC+SD)$ versus cloud amount for cirrus clouds with thickness of 1 km and five different cloud-top altitudes from 7 to 11 km.

itself induces a weak negative feedback. The sensitivity parameter ratio $R(SD)$ has a minimum value at the cloud top altitude of 10 km where the size distribution of the cirrus cloud changes drastically. The value of the sensitivity parameter ratio $R(IWC+SD)$, which includes both IWC and size distribution feedbacks, shows that the combined effect of the two feedbacks generally induces a weak positive feedback except for cloud top altitude of 10 km. The negative size distribution feedback obviously weakens the positive IWC feedback at the cloud top altitudes of 8, 10 and 11 km, though the negative feedback induced by the change of size distribution ($R(SD)$) is very weak. This curious behavior of the size distribution feedback arises from a non-linearity of the feedback processes. At the cloud-top altitude of 10 km, the IWC feedback is offset by the size-distribution feedback, so that the cirrus cloud microphysics induces no climate feedback. The sensitivity parameter ratio $R(H_2O+IWC+SD)$ which includes the water vapor, IWC and size distribution feedbacks simultaneously, ranges from 1.5 to 4.2. The microphysical feedback of cirrus clouds drastically enhances the positive water vapor feedback at the cloud-top altitudes from 7 to 11 km except for 10 km. In the above discussion, however, the accuracy of $R(H_2O+IWC+SD)$ should be examined at lower cloud top altitudes where the ratio $R(H_2O+IWC+SD)$ takes large values, because small errors of partial derivatives affect significantly the calculated value in this case. This point will be discussed in Section 5.3.

As mentioned in Section 4.1.2, cirrus clouds have various thicknesses from 0.1 to 8 km. The sensitivity parameter ratios are also calculated for overcast cirrus clouds with thicknesses of 2 and 3 km. In these cases, the values of $\partial H/\partial[IWC]\times\partial[IWC]/\partial T$ are ranging from 1.9 to 2.3 W m^{-2}°C^{-1}, and the values of $\partial H/\partial[SD]\times\partial[SD]/\partial T$ are ranging from -0.2 to -1.5 W m^{-2}°C^{-1}. Thus, the positive IWC feedback exceeds the negative size distribution feedback, so that the total microphysical feedback is positive for both cloud thicknesses of 2 and 3 km. Figure 6 shows the sensitivity parameter ratio $R(H_2O+IWC+SD)$ which includes the water vapor, the IWC and the size distribution feedbacks simultaneously, for cloud thicknesses from 1 to 3 km. The values of the ratio are larger for clouds thicknesses of 2 and 3 km than those for cloud thickness of 1 km, except for the cloud top altitude of 11 km. Such large values of $R(H_2O+IWC+SD)$ result from the large positive IWC feedback for thicker clouds. The clouds of 2 and 3 km thickness show rather small values of $R(H_2O+IWC+SD)$ at cloud top altitudes of 10 and 11 km. This result reflects the effect of drastic change of size distribution at a cloud temperature around -45°C.

The magnitude of the microphysical feedback of cirrus clouds is so far estimated for overcast conditions. The sensitivity parameter ratio for partially cloudy conditions, $R_{PC}(H_2O+IWC+SD)$, is shown in Fig. 7 as a function of the cloud amount which is assumed to be constant throughout the climate change. A single cirrus cloud layer of thickness 1 km is embedded at the cloud-top altitudes from 7 to 11 km. The values of $R_{PC}(H_2O+IWC+SD)$ increase with increasing cloud amount, except

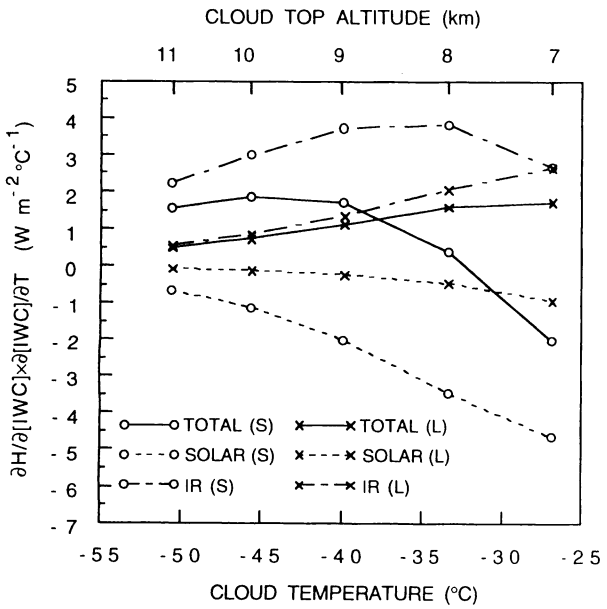

Fig. 8. Partial derivatives related to ice water content feedback (solid line), its solar component (broken line) and infrared component (dash-dot line) for fixed size distributions S and L.

for the cloud top altitude of 10 km. The globally-averaged value of the cirrus cloud amount is about 0.2 for the current climate (Warren *et al.*, 1988). If we assume this cloud amount (*i.e.*, 0.2) is kept unchangeable throughout the climate change, the value of $R_{PC}(H_2O+IWC+SD)$ is estimated to be about 1.8, except for the cloud top altitude of 10 km. The sensitivity parameter ratio $R_{PC}(H_2O)$ is calculated to be about 1.6 for the same cloud amount of 0.2. Such results are quite similar for cloud thicknesses of 2 and 3 km. The global warming of 1.2°C due to the direct effect of CO_2 doubling (ΔT_0) (*e.g.*, Schlesinger and Mitchell, 1987) is therefore amplified to about 2.2°C and 1.9°C by $R_{PC}(H_2O+IWC+SD)$ and $R_{PC}(H_2O)$, respectively, for the cloud amount of 0.2.

5. Discussion

5.1 *Influence of initial states of the atmosphere on microphysical feedbacks of cirrus cloud*

The magnitudes of the microphysical feedback of cirrus clouds depend not only on changes of microphysical quantities due to the temperature change but also on the initial states of the atmosphere. In order to examine the effect of initial size distributions on the partial derivatives $\partial H/\partial[IWC]\times\partial[IWC]/\partial T$, two size distributions are chosen as representatives of small and large particle sizes; one is the size distribution for the temperature range of −50−−55°C (S), and the other is that for the temperature range of −25−−30°C (L). The effective

Table 2. Upward effective emissivity of cirrus cloud evaluated at each cloud-top altitude for two fixed size distributions: size distribution in the temperature range from −50 to −55°C (S distribution); size distribution in the temperature range from −25 to −30°C (L distribution). Upward effective emissivity $\varepsilon_0^{\uparrow}$ is calculated with the initial state of the model atmosphere, and $\varepsilon_{\delta IWC}^{\uparrow}$ is evaluated with the model atmosphere in which only cirrus cloud IWC increases in response to a tropospheric temperature increase of 5°C. Also presented is the change of upward effective emissivity $\Delta\varepsilon^{\uparrow}$ which is defined by the difference between $\varepsilon_0^{\uparrow}$ and $\varepsilon_{\delta IWC}^{\uparrow}$.

Cloud top altitude (km)	$\varepsilon_0^{\uparrow}$	$\varepsilon_{\delta IWC}^{\uparrow}$	$\Delta\varepsilon^{\uparrow}$
	S distribution		
11	0.15	0.23	0.08
10	0.24	0.35	0.11
9	0.37	0.52	0.15
8	0.58	0.75	0.17
7	0.80	0.93	0.13
	L distribution		
11	0.06	0.08	0.02
10	0.09	0.12	0.03
9	0.14	0.19	0.05
8	0.23	0.32	0.09
7	0.37	0.50	0.13

radii are 24 and 104 μm for the respective size distributions (see Fig. 2). These size distributions are assumed to be independent of the altitude (temperature) of the cirrus cloud. A 1 km-thick cirrus cloud is embedded. The dependence of $\partial H/\partial[IWC]\times\partial[IWC]/\partial T$ on the cloud-top altitude changes drastically with the size distribution of cloud particles as shown in Fig. 8. The value of $\partial H/\partial[IWC]\times\partial[IWC]/\partial T$ for the total radiation increases monotonically with decreasing altitude for the L distribution, while it takes a maximum at the cloud-top altitude of 10 km, and changes its sign at the cloud-top altitude near 8 km for the S distribution. As a result, the total $\partial H/\partial[IWC]\times\partial[IWC]/\partial T$ for the S distribution has a larger value than that for the L distribution at lower temperatures, and vice-versa at higher temperatures. For the infrared radiation, the values of $\partial H/\partial[IWC]\times\partial[IWC]/\partial T$ for the S distribution are larger than those for the L distribution, except for the cloud top altitude of 7 km. The value of $\partial H/\partial[IWC]\times\partial[IWC]/\partial T$ for the infrared radiation depends on the cloud temperature itself as well as the change of cloud emissivity due to the change of IWC. The values of $\partial H/\partial[IWC]\times\partial[IWC]/\partial T$ for the infrared radiation are expected

to increase monotonically with increasing temperature, if the change of cloud emissivity is kept constant or increases with the cloud temperature. In the case of the S distribution, however, the value of $\partial H/\partial[IWC]\times\partial[IWC]/\partial T$ for the infrared radiation turns to decrease with decreasing cloud altitude below 8 km. In order to examine the effect of cirrus cloud emissivity on $\partial H/\partial[IWC]\times\partial[IWC]/\partial T$, the change of upward effective emissivity is calculated at each cloud-top altitude as shown in Table 2. The upward effective emissivity is defined according to Cox (1976) as

$$\varepsilon^{\uparrow}=\frac{F_B^{\uparrow}-F_T^{\uparrow}}{F_B^{\uparrow}-\sigma T_T^4}, \tag{16}$$

where $F^{\uparrow}$ is the upward infrared radiative flux, T is the temperature, the subscripts T and B refer to the top and bottom of the cloud layer, respectively, and σ is the Stefan-Boltzmann constant. The altitude dependence of the change of effective emissivity, $\Delta\varepsilon^{\uparrow}$, is quite similar to that of $\partial H/\partial[IWC]\times\partial[IWC]/\partial T$ for the infrared radiation in both cases of the S and L distributions: the value of $\partial H/\partial[IWC]\times\partial[IWC]/\partial T$ for the infrared radiation reaches a maximum at the same altitude where the change of effective emissivity has a maximum value for the S distribution. Thus, the cirrus cloud emissivity plays an important rôle in determining the value of $\partial H/\partial[IWC]\times\partial[IWC]/\partial T$. For the solar radiation, the quantity $\partial H/\partial[IWC]\times\partial[IWC]/\partial T$ has a smaller negative value for the L distribution than for the S distribution, especially at lower altitudes (or higher temperatures). The value of $\partial H/\partial[IWC]\times\partial[IWC]/\partial T$ for the solar radiation depends on the change of cloud albedo due to the change of IWC. The increase of the cloud albedo with an increase of IWC becomes less significant as the particle sizes increase. It is therefore concluded that the temperature dependence of the size distribution tends to make the IWC feedback positive: the S distribution enhances the positive value of $\partial H/\partial[IWC]\times\partial[IWC]/\partial T$ for the infrared radiation (positive feedback) at lower temperatures, and the L distribution suppresses the negative values of $\partial H/\partial[IWC]\times\partial[IWC]/\partial T$ for the solar radiation (negative feedback) at higher temperatures.

Similarly, the value of $\partial H/\partial[SD]\times\partial[SD]/\partial T$ depends on the initial value of IWC. Fig. 9 shows the partial derivatives $\partial H/\partial[SD]\times\partial[SD]/\partial T$ for the total radiation taking the ice water path (IWP) as a parameter, where IWP is the total amount of ice water content included in the vertical cloud column. The values of 1.5, 5.1 and 22.4 g m^{-2} correspond to the IWP values of 1 km-thick cirrus clouds with the cloud top altitudes of 11, 9 and 7 km, respectively. The relation between $\partial H/\partial[SD]\times\partial[SD]/\partial T$ and the initial value of the IWP is

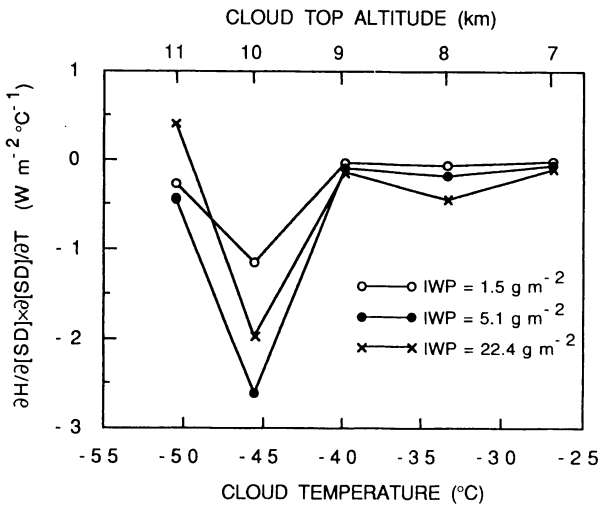

Fig. 9. Partial derivatives related to size distribution feedback for fixed ice water contents.

not monotonous at cloud- top altitudes of 10 and 11 km, though the absolute values of $\partial H/\partial[SD]\times\partial[SD]/\partial T$ for both solar and infrared radiations increase monotonically with increasing IWP at all cloud top altitudes. This is because the positive value of $\partial H/\partial[SD]\times\partial[SD]/\partial T$ for the solar radiation increases more rapidly than the negative value of $\partial H/\partial[SD]\times\partial[SD]/\partial T$ for the infrared radiation with increasing IWP at these altitudes. The result in Fig. 9 is quite similar to the altitude dependence of $\partial H/\partial[SD]\times\partial[SD]/\partial T$ for the total radiation shown in Fig. 4. The largest negative values of $\partial H/\partial[SD]\times\partial[SD]/\partial T$ appear at the cloud-top altitude of 10 km for all values of IWP. Thus, it is clear that the large size distribution feedback for the cirrus cloud with top altitude of 10 km results, not from the difference of the initial IWC value but from the drastic change of the size distribution itself.

5.2 Effect of crystal shape on microphysical feedbacks of cirrus clouds

Theoretical calculations show that single-scattering properties of columns (cylinders) are considerably different from those of equivalent Mie spheres (Takano and Liou, 1989; Stephens, 1980). The effect of crystal shape may be significant, especially for the solar spectral region where the values of the size parameter are very large. Stackhouse and Stephens (1991) showed that the observed albedo of cirrus clouds increases more rapidly with increasing IWP than the albedo calculated for model clouds with Mie particles, though the agreement between measured and calculated emissivities is fairly good. They suggested that such a discrepancy in the cloud albedo would be consistently explained by the crystal shape effect. The non-sphericity of cloud particles enhances the increase of cirrus albedo with in-

creasing IWC and, thus, increases the magnitude of the IWC feedback for the solar radiation. This is because the asymmetry factor of the phase function is considerably smaller for the non-spherical particles than for the equivalent Mie particles. Stackhouse and Stephens (1991) showed that the most plausible value of the asymmetry factor is 0.7 for realistic cirrus instead of the calculated value of around 0.87 for equivalent Mie particles, and that the rate of increase of the cirrus albedo due to the increase of IWP is larger by about 2.5 times for the cirrus cloud with the asymmetry factor of 0.7 than for the cirrus cloud with the asymmetry factor of 0.87. Because the value of $\partial H/\partial[IWC]\times\partial[IWC]/\partial T$ for the solar radiation is expected to be nearly proportional to the change of cloud albedo due to the change of IWP, the non-sphericity of cloud particles amplifies the value of $\partial H/\partial[IWC]\times\partial[IWC]/\partial T$ for the solar radiation by a factor of about 2.5. Assuming this amplification factor of 2.5 in the solar spectral region, the values of $\partial H/\partial[IWC]\times\partial[IWC]/\partial T$ for the total radiation discussed in Section 4.2 become 0.3–0.9 $\mathrm{W\,m^{-2}{}^{\circ}C^{-1}}$ for 1 km-thick cloud, −0.2–0.8 $\mathrm{W\,m^{-2}{}^{\circ}C^{-1}}$ for 2 km-thick cloud and −0.5–−0.2 $\mathrm{W\,m^{-2}{}^{\circ}C^{-1}}$ for 3 km-thick cloud: the effect of crystal shape reduces the positive IWC feedback to bring about a negative feedback for the thick cirrus.

The value of $\partial H/\partial[SD]\times\partial[SD]/\partial T$ for the solar radiation is also expected to be proportional to the change of cirrus albedo due to the change of the size distribution (effective radius). Stephens *et al.* (1990) showed the relationship between the albedo and the effective radius of cirrus particles for two values of the asymmetry factor of 0.7 and 0.87. The former corresponds to non-spherical particles and the latter to equivalent Mie spheres. The changes of albedo due to the change of effective radius are similar to each other for these two cases of the asymmetry factor. This result suggests that the effect of crystal shape on the size distribution feedback may be relatively small. However, the effect of crystal shape on the size distribution feedback is complicated, because both the size distribution and the particle shape affect not only the extinction coefficient but also the single-scattering albedo and the phase function in a complicated manner. Single-scattering properties of various ice crystals should be studied more comprehensively to investigate microphysical feedbacks of cirrus clouds more quantitatively.

5.3 Influence of the choice of model atmospheres

In Section 3, the sensitivity parameter ratio is introduced on the assumption that ΔH vanishes at both the initial and final states, climate system being in equilibrium at both states. The model atmospheres used for evaluating the sensitivity parameter ratio, however, do not satisfy this condition. If

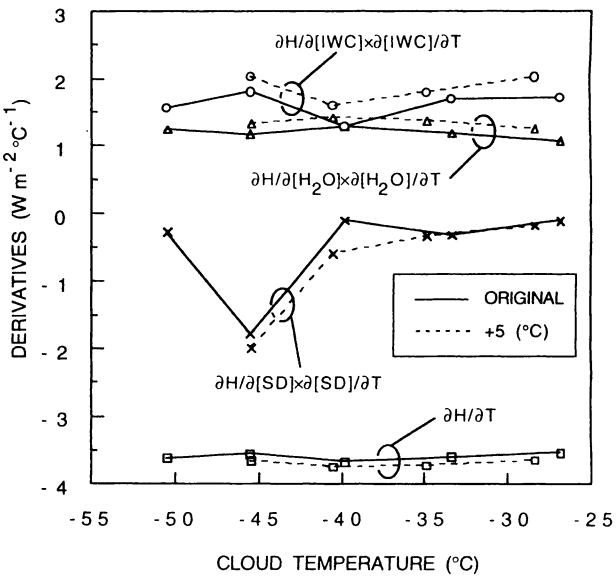

Fig. 10. Partial derivatives related to respective feedbacks versus cloud temperature for the original model atmosphere (solid lines) and a model atmosphere with a tropospheric temperature higher by 5°C than the original model atmosphere (broken lines).

the values of the partial derivatives related to each feedback mechanism are sensitive to the choice of model atmospheres, the sensitivity parameter ratio cannot be estimated accurately by utilizing such model atmospheres. Therefore, the sensitivity of these quantities to the choice of model atmospheres should be investigated to examine the validity of climate feedbacks evaluated in this study. Because our model atmospheres do not include middle and low clouds which decrease the equilibrium temperature significantly, model atmospheres to be served for evaluating cirrus cloud feedbacks should be those with higher equilibrium temperatures than the atmosphere of Manabe and Wetherald (1967). In order to investigate the influence of the choice of model atmospheres on the magnitude of the feedbacks evaluated in this study, the partial derivatives and the sensitivity parameter ratios related to each feedback mechanism are calculated with the initial temperature profile which is 5°C higher in the troposphere than the original temperature profile of Manabe and Wetherald (1967). The initial values of other parameters such as water vapor concentration, IWC and size distribution are also changed from their original initial values, corresponding to the increase of the initial temperature. Absolute values of the partial derivatives obtained with this new initial condition are slightly larger than those obtained with the original temperature profile, as shown in Fig. 10. It is found that the choice of model atmospheres slightly

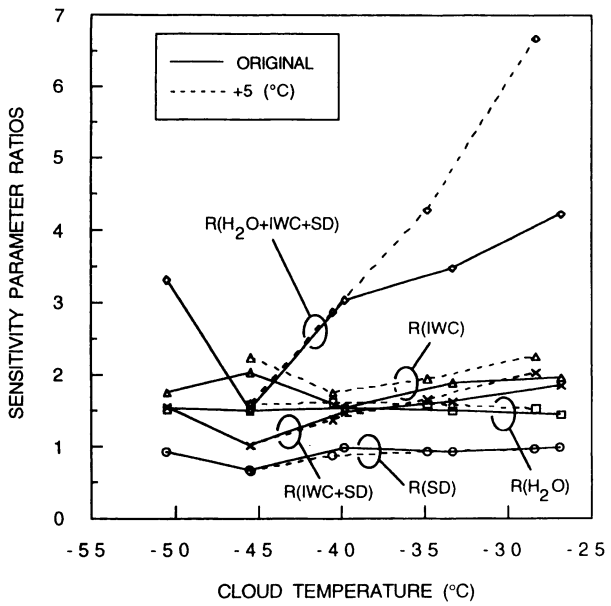

Fig. 11. Same as Fig. 10, except for the sensitivity parameter ratios.

influences the partial derivatives for each feedback mechanism. The sensitivity parameter ratios for both initial temperature profiles are almost same as each other except for the ratio $R(H_2O+IWC+SD)$ at higher temperatures, as shown in Fig. 11. The absolute values of the sensitivity parameter $\lambda(H_2O+IWC+SD)$ are smaller than the absolute values of the respective partial derivatives for direct temperature response, the water vapor feedback and the IWC feedback at higher temperatures. In such cases, small differences between each pair of partial derivatives shown in Fig. 10 cause a large difference in the sensitivity parameter $\lambda(H_2O+IWC+SD)$, and the sensitivity parameter ratio $R(H_2O+IWC+SD)$ becomes more sensitive to the choice of model atmospheres. Careful treatment is therefore necessary, especially to evaluate the magnitudes of strong feedback.

5.4 Cirrus cloud feedback in the tropics

Recently, Ramanathan and Collins (1991) discussed the cirrus cloud feedback in the tropics. They claimed that the sea surface temperature (SST) in the tropics may be limited to less than 305 K by the negative feedback of cirrus clouds due to spreading of thick anvil clouds which reflect the solar radiation back to space. They analyzed the radiation budget data from the Earth Radiation Budget Experiment (ERBE) and the SST data from weather satellites and ships, and estimated the derivatives dC_s/dT and dC_l/dT to examine the magnitude of the cirrus cloud feedback, where C_s and C_l are cloud radiative forcings for short-wave and long-wave radiations, respectively. The values of dC_s/dT and dC_l/dT which they estimated are in the range from -22 to -27 $\mathrm{W\,m^{-2}{}^{\circ}C^{-1}}$ and from 18 to 23 $\mathrm{W\,m^{-2}{}^{\circ}C^{-1}}$, respectively.

This negative feedback comes mainly from the changes of both microphysical and macrophysical properties of cirrus clouds. To make clear the influence of IWC on the derivatives dC_s/dT and dC_l/dT for the tropical cirrus clouds, we estimate the quantities $\partial C_s/\partial[IWC]\times\partial[IWC]/\partial T$ and $\partial C_l/\partial[IWC]\times\partial[IWC]/\partial T$ by model calculations with the radiative transfer code described in Section 4.1.1. The cloud radiative forcing C_s (or C_l) is calculated as a product of the cloud amount by the difference of net short-wave (or long-wave) flux at the top of the atmosphere between clear and overcast conditions. The model cirrus cloud is assumed as follows, though microphysical and macrophysical properties of the tropical cirrus cloud investigated by Ramanathan and Collins (1991) are not clear. A cirrus cloud layer of 1 km thickness is embedded at the cloud top altitude of 11 km. The size distribution is fixed to that for the temperature range from -50 to -55°C. The initial value of the IWP is assumed to be 50 $\mathrm{g\,m^{-2}}$, according to the vertical distribution of IWC in the tropical cirrus clouds observed by Griffith *et al.* (1980). The optical thickness of this model cirrus is 4.2 at the wavelength of 0.6 μm. This value is consistent with the observed visible optical thickness of tropical cirrus ranging from 0.5 to more than 6 (Liou *et al.*, 1990). The rate of increase of IWP with increasing temperature is adopted within the range from 0.5 to 5 $\mathrm{g\,m^{-2}{}^{\circ}C^{-1}}$. These values of increasing rate of IWP correspond to that of the model cirrus clouds embedded in the model tropical atmosphere with the cloud top altitude of 11 km and thicknesses ranging from 1 to 3 km, if the value of IWC is given from the parameterization in Section 2.1. The same model tropical atmosphere as used in LOWTRAN7 is adopted, and the surface albedo and the cosine of the solar zenith angle are assumed to be 0.1 and 0.64, respectively. On these assumptions, the values of $\partial C_s/\partial[IWC]\times\partial[IWC]/\partial T$ and $\partial C_l/\partial[IWC]\times\partial[IWC]/\partial T$ are estimated in the range from -0.6 to -5.7 $\mathrm{W\,m^{-2}{}^{\circ}C^{-1}}$ and from 0.2 to 1.6 $\mathrm{W\,m^{-2}{}^{\circ}C^{-1}}$, respectively, for overcast condition. The absolute values of these derivatives are smaller for partially cloudy conditions than for overcast conditions. The magnitude of the feedback mechanism through the change of IWP is therefore too small to explain the observed values, even if the effect of ice crystal shape discussed in Section 5.2 is taken into account. The influence of cloud amount (CA) on both derivatives, dC_s/dT and dC_l/dT, is also evaluated by using the same models. The values of $\partial C_s/\partial[CA]\times\partial[CA]/\partial T$ and $\partial C_l/\partial[CA]\times\partial[CA]/\partial T$ are estimated to be -8.8 $\mathrm{W\,m^{-2}{}^{\circ}C^{-1}}$ and 13.6 $\mathrm{W\,m^{-2}{}^{\circ}C^{-1}}$, respectively, for an increasing rate of cloud amount of $0.1\,^{\circ}\mathrm{C}^{-1}$ estimated from the nephanalysis data of Gadgil *et al.*

(1984).

These comparisons between observations and theoretical calculations suggest that the change of cloud amount is also very important for the tropical climate as well as the change of microphysical properties. Though the effect of microphysical feedback of cirrus cloud is not so significant at least for the current global average cloud amount as discussed in Section 4.2.2, cirrus clouds are still expected to induce a significant climate feedback by the combination of the macrophysical and microphysical feedback mechanisms.

6. Summary

The microphysical feedback of cirrus clouds has been investigated by use of a newly developed radiation code which can treat radiative transfer in realistic atmospheres with reasonable accuracy for both solar and infrared radiations. The ice water content (IWC) and the size distribution of cirrus clouds are parameterized in terms of the cloud temperature from airborne measurement data. Both of the IWC and the size distribution feedbacks are evaluated in terms of the sensitivity parameter ratios and related partial derivatives.

Model cirrus clouds with thicknesses from 1 to 3 km and cloud top altitudes from 7 to 11 km are adopted to evaluate the magnitudes of the microphysical feedback processes. The temperature dependence of the IWC induces the derivatives $\partial H/\partial[IWC]\times\partial[IWC]/\partial T$ in the range from 1.3 to $2.3\,\mathrm{W\,m^{-2}{}^{\circ}C^{-1}}$, which causes a positive feedback. The temperature dependence of the size distribution, on the other hand, induces the derivatives $\partial H/\partial[SD]\times\partial[SD]/\partial T$ in the range from -0.1 to $-1.8\,\mathrm{W\,m^{-2}{}^{\circ}C^{-1}}$, which causes a negative feedback. The positive IWC feedback exceeds the negative size distribution feedback, so that the microphysical feedback of cirrus clouds is positive as a net effect. The sensitivity parameter ratio indicates, however, that the IWC feedback is weakened significantly by the size distribution feedback, especially for a cloud temperature near -45°C. The temperature dependence of the size distribution not only induces a feedback effect by itself but also affects the magnitude of the IWC feedback. The size distribution enriched with smaller particles at lower temperatures enhances the positive IWC feedback for the infrared radiation, while the size distribution enriched with larger particles at higher temperatures suppresses the negative IWC feedback for the solar radiation. For partially cloudy conditions with cloud amount of 0.2, the sensitivity parameter ratio increases from about 1.6 to about 1.8 due to the microphysical feedback of cirrus clouds. This increase of the sensitivity parameter ratio by about 0.2 amplifies the global warming due to CO_2 doubling by about 0.3°C. The importance of investigating the feedback mechanism due to the change of macrophysical properties of cirrus clouds is also pointed out.

Acknowledgements

The authors would like to thank Dr. G. Y. Shi for kindly providing the new ESFT parameters, and Dr. T. Hayasaka for giving valuable comments.

References

Cess, R.D., G.L. Potter, J.P. Blanchet, G.J. Boer, A.D. Del Genio, M. Déqué, V. Dymnikov, V. Galin, W.L. Gates, S.J. Ghan, J.T. Kiehl, A.A. Lacis, H. Le Treut, Z.-X. Li, X.-Z. Liang, B.J. McAvaney, V.P. Meleshko, J.F.B. Mitchell, J.-J. Morcrette, D.A. Randall, L. Rikus, E. Roeckner, J.F. Royer, U. Schlese, D.A. Sheinin, A. Slingo, A.P. Sokolov, K.E. Taylor, W.M. Washington, R.T. Wetherald, I. Yagai and M.-H. Zhang, 1990: Intercomparison and interpretation of climate feedback processes in 19 atmospheric general circulation models. *J. Geophys. Res.*, **95**, 16601–16615.

Charlock, T.P., 1982: Cloud optical feedback and climate stability in a radiative-convective model. *Tellus*, **34**, 245–254.

Cox, S.K., 1976: Observations of cloud infrared effective emissivity. *J. Atmos. Sci.*, **33**, 287–289.

Dowling, D.R. and L.F. Radke, 1990: A summary of the physical properties of cirrus clouds. *J. Apple. Meteor.*, **29**, 970–978.

Foot, J.S., 1988: Some observations of the optical properties of clouds. II: Cirrus. *Quart. J. Roy. Meteor. Soc.*, **114**, 145–164.

Fröhlich, C. and J. London, 1986: Revised instruction manual on radiation instruments and measurements, WCRP publications series No. 7, WMO/TD-No. 149, 140 pp.

Gadgil, S., P.V. Joseph and N.V. Joshi, 1984: Ocean-atmosphere coupling over monsoon region. *Nature*, **312**, 141–143.

Griffith, K.T., S.K. Cox and R.G. Knollenberg, 1980: Infrared radiative proprieties of tropical cirrus clouds inferred from aircraft measurements. *J. Atmos. Sci.*, **37**, 1077–1087.

Heymsfield, A.J., 1972: Ice crystal terminal velocities. *J. Atmos. Sci.*, **29**, 1348–1357.

Heymsfield, A.J., 1977: Precipitation development in stratiform ice clouds: A microphysical and dynamical study. *J. Atmos. Sci.*, **34**, 367–381.

Heymsfield, A.J. and C.M.R. Platt, 1984: A parameterization of the particle size spectrum of ice clouds in terms of the ambient temperature and the ice water content. *J. Atmos. Sci.*, **41**, 846–855.

Heymsfield, A.J. and L.J. Donner, 1990: A scheme for parameterizing ice-cloud water content in general circulation models. *J. Atmos. Sci.*, **47**, 1865–1877.

Liou, K.-N., Q. Fu and T.P. Ackerman, 1988: A simple formulation of the delta-four-stream approximation for radiative transfer parameterizations. *J. Atmos. Sci.*, **45**, 1940–1947.

Liou, K.-N., S.C. Ou, Y. Takano, F.P.J. Valero and T.P. Ackerman, 1990: Remote sounding of the tropical cirrus cloud temperature and optical depth using 6.5 and 10.5 μm radiometers during STEP. *J. Appl. Meteor.*, **29**, 716–726.

Manabe, S. and R.T. Wetherald, 1967: Thermal equilibrium of the atmosphere with a given distribution of relative humidity. *J. Atmos. Sci.*, **24**, 241–259.

Nakajima, T. and M. Tanaka, 1986: Matrix formulations for the transfer of solar radiation in a plane-parallel scattering atmosphere. *J. Quant. Spectrosc. Radiat. Transfer*, **35**, 13–21.

Ramanathan, V. and W. Collins, 1991: Thermodynamic regulation of ocean warming by cirrus clouds deduced from observations of the 1987 El Niño. *Nature*, **351**, 27–32.

Roberts, R.E., J.E.A. Selby and L.M. Biberman, 1976: Infrared continuum absorption by atmospheric water vapor in the 8–12-μm window. *Appl. Opt.*, **15**, 2085–2090.

Roeckner, E., U. Schlese, J. Biercamp and P. Loewe, 1987: Cloud optical depth feedbacks and climate modelling. *Nature*, **329**, 138–140.

Sassen, K., D.O'C. Starr and T. Uttal, 1989: Mesoscale and microscale structure of cirrus clouds: Three case studies. *J. Atmos. Sci.*, **46**, 371–396.

Schlesinger, M.E. and J.F.B. Mitchell, 1987: Climate model simulations of the equilibrium climatic response to increased carbon dioxide. *Rev. Geophys.*, **25**, 760–798.

Schlesinger, M.E. and E. Roeckner, 1988: Negative or positive cloud optical depth feedback. *Nature*, **335**, 303–304.

Shi, G.Y., 1981: An accurate calculation and representation of the infrared transmission function of the atmospheric constituents. Ph.D. thesis, Tohoku University.

Slingo, A., 1990: Sensitivity of the earth's radiation budget to changes in low clouds. *Nature*, **343**, 49–51.

Somerville, R.C.J. and L.A. Remer, 1984: Cloud optical thickness feedbacks in the CO_2 climate problem. *J. Geophys. Res.*, **89**, 9668–9672.

Stackhouse, Jr., P.W. and G.L. Stephens, 1991: A theoretical and observational study of the radiative properties of cirrus: Results from FIRE 1986. *J. Atmos. Sci.*, **48**, 2044–2059.

Stephens, G.L., 1980: Radiative properties of cirrus clouds in the infrared region. *J. Atmos. Sci.*, **37**, 435–446.

Stephens, G.L., S.-C. Tsay, P.W. Stackhouse, Jr. and P.J. Flatau, 1990: The relevance of the microphysical and radiative properties of cirrus clouds to climate and climatic feedback. *J. Atmos. Sci.*, **47**, 1742–1753.

Takano, Y. and K.-N. Liou, 1989: Solar radiative transfer in cirrus clouds. Part I: Single-scattering and optical properties of hexagonal ice crystals. *J. Atmos. Sci.*, **46**, 3–19.

Warren, S.G., 1984: Optical constants of ice from the ultraviolet to the microwave. *Appl. Opt.*, **23**, 1206–1225.

Warren, S.G., C.J. Hahn, J. London, R.M. Chervin and R.L. Jenne, 1988: Global distribution of total cloud cover and cloud type amounts over the ocean. NCAR Tech. Notes, NCAR/TN-317+STR, 42 pp.

Wiscombe, W.J., 1977: The delta-M method: Rapid yet accurate radiative flux calculations for strongly asymmetric phase functions. *J. Atmos. Sci.*, **34**, 1408–1422.

World Meteorological Organization, 1985: Atmospheric ozone 1985, Global ozone research and monitoring project, Rep. 16, Geneva.

気候変動における巻雲の微物理過程のフィードバック

鈴木恒明・田中正之
(東北大学理学部大気海洋変動観測研究センター)
中島映至
(東京大学気候システム研究センター)

巻雲の雲氷量と粒径分布の温度依存性を考慮して、気候変動における巻雲のフィードバック効果を調べた。偏微分の和として定義される敏感度パラメーターを、4ストリームのディスクリート－オーディネイト法とESFT法を用いて作成した高精度の放射コードで計算した。その際、飛行機観測データに基づいて雲氷量と粒径分布を温度でパラメーター化し、これを用いて微物理量の温度依存性を考慮した。雲氷量のフィードバックに関係した偏微分 $\partial H/\partial[IWC] \times \partial[IWC]/\partial T$ の値は 1.3–2.3W $m^{-2}°C^{-1}$ であり、雲氷量の温度依存性は正のフィードバックを引き起こす。一方、粒径分布に関係した偏微分 $\partial H/\partial[SD] \times \partial[SD]/\partial T$ の値は -0.1–-1.8W $m^{-2}°C^{-1}$ であり、これは粒径分布の温度依存性によるフィードバックが負であることを意味する。特に巻雲が $-45°C$ 付近に存在する場合、雲氷量の正のフィードバックは粒径分布の負のフィードバックによって相殺される。雲氷量のみならず粒径分布の温度依存性が巻雲の微物理過程のフィードバックの評価において重要であることを示した。